The Astrophysical Journal Supplement Series, 263:3 (14pp), 2022 November https://doi.org/10.3847/1538-4365/ac9183

REST: A Java Package for Crafting Realistic Cosmic Dust Particles

Prithish Halder
Indian Institute of Astrophysics, Koramangala, Bengaluru, Karnataka 560034, India; prithishh3@gmail.com, prithish.halder@iiap.res.in
Received 2022 July 25; revised 2022 September 7; accepted 2022 September 11; published 2022 October 21

Abstract

The overall understanding of cosmic dust particles is mainly inferred from the different Earth-based measurements of interplanetary dust particles and space missions such as Giotto, Stardust, and Rosetta. The results from these measurements indicate the presence of a wide variety of morphologically significant dust particles. To interpret the light-scattering and thermal emission observations arising due to dust in different regions of space, it is necessary to generate computer-modeled realistic dust structures of various shapes, sizes, porosity, bulk density, aspect ratio, and material inhomogeneity. The present work introduces a Java package called Rough Ellipsoid Structure Tool (REST), which is a collection of multiple algorithms, that aims to craft realistic rough-surface cosmic dust particles from spheres, superellipsoids, and fractal aggregates depending on the measured bulk density and porosity. Initially, spheres having N_d dipoles or lattice points are crafted by selecting random material and space seed cells to generate a strongly damaged structure, rough surface, and poked structure. Similarly, REST generates rough-surface superellipsoids and poked structure superellipsoids from initial superellipsoid structures. REST also generates rough fractal aggregates, which are fractal aggregates having rough-surface irregular grains. REST has been applied to create agglomerated debris, agglomerated debris superellipsoids, and mixed-morphology particles. Finally, the light-scattering properties of the respective applied structures are studied to ensure their applicability. REST is a flexible structure tool that shall be useful for generating various types of dust structures that can be applied to studying the physical properties of dust in different regions of space.

Unified Astronomy Thesaurus concepts: Dust physics (2229); Interplanetary dust (821); Circumstellar dust (236); Interstellar dust (836); Radiative transfer simulations (1967); Software available on request (1865)

1. Introduction

Signatures of dust particles can be found in almost every corner of the visible universe. The physics of dust plays a crucial role in the understanding of the formation and evolution of galaxies as dust particles in a galaxy interact with dust, gas, stars, and dark matter under the effect of radiation pressure, magnetic fields, and gravity (Bekki 2015). In most of the studies, the structure of dust is either considered to be spherical or spheroidal in nature, while in reality, dust particles can have different kinds of shapes depending on the effect of different forces. The studies related to comet dust and/or atmospheric dust consider the most complex morphology for the associated dust particles in order to compensate the detailed observations of the structures. Various groundbreaking studies such as those of interplanetary dust particles (IDPs) collected from both the Antarctic ice and the Earth's stratosphere (Brownlee 1985; Lawler & Brownlee 1992; Bradley 2007; Noguchi et al. 2015), the dust particles collected from the Stardust mission (Hörz et al. 2006), and the microphysical measurements of dust by the Rosetta/MIDAS and COSIMA instruments (Güttler et al. 2019; Mannel et al. 2019) prepare a detailed picture of the physical parameters associated with dust particles that are beyond the spherical geometry. Thus, dust particles found in space are not just simple spheres or spheroids, rather they have complex geometries and can be categorized into several groups, namely fractal aggregates, agglomerated debris, rough spheroids, Gaussian random spheres, etc. Researchers have often used such complex structures to model the light-scattering and thermal emission observations of aerosols, comets, asteroids, protoplanetary disks, and debris disks (Kimura et al. 2006; Das et al. 2011; Kolokolova et al. 2015; Deb Roy et al. 2017; Halder et al. 2018; Muinonen et al. 2019; Choudhury et al. 2020; Zubko et al. 2020; Halder & Ganesh 2021; Aravind et al. 2022; Petrov & Zhuzhulina 2022; Zhuzhulina et al. 2022). Rigorous numerical techniques are required to construct such complex irregular structures. In recent years materials scientists from different fields such as atmospheric physics and nanophysics have introduced superspheroids and/or superellipsoids into their studies in order to model the observed optical response from such complex structures. Superellipsoids are highly generalized geometrical structures whose shape depends on the aspect ratio, north–south, and east–west components defined by Equation (1) in Section 2.4. Lin et al. (2018) used superellipsoids to model the measured light-scattering properties of 25 samples of dust particles (collected from different arid regions on Earth) from the Amsterdam–Granada Light Scattering Database (Muñoz et al. 2012). On the other hand, Chatterjee et al. (2021) used superellipsoids to study the variation of plasmonic sensing with the changing morphology of nanoparticles. Application of superellipsoids in the study of astrophysical dust shall provide simpler solutions despite the dust having irregular geometry. With the evolution of interpretations of cosmic dust properties from spherical → spheroidal → irregular, the related light-scattering theories have also evolved. For example, the Mie scattering theory that is applicable to single spheres has evolved into T-matrix theory (Waterman 1971; Mishchenko et al. 1996; Bi et al. 2013, 2022) and discrete dipole approximation (Purcell et al. 1973; Draine & Flatau 1994; Yurkin & Hoekstra 2011), which are applicable to arbitrary and/or highly irregular dust structures.

Various applications have emerged to configure and generate ballistic aggregates, ellipsoids, cubes, rectangular blocks, etc., but there are negligible applications generating rough or irregular geometries. This led us to the development of the Rough Ellipsoid Structure Tools (REST) package that can generate rough-surface structures (RS), poked structures (PS), and agglomerated debris (AD) out of ellipsoids and super-ellipsoids. Apart from the single particle structures REST also generates rough fractal aggregates (RFA), which are fractal aggregates having rough-surface irregular grains/monomers from fractal aggregates of spheres (FA). The development of the package, the input and output parameters, and algorithm for the different structures are discussed in Section 2. The physical parameters associated with the structures are explained in Section 3. Some selected applications of REST and related light-scattering results are depicted in Section 4.

The instructions related to the basic usage of REST are provided in the online documentation.[1] REST will become publicly available through the online documentation link in due course. An online request form[2] related to accessing different structures generated using REST is available in the online documentation. The request form provides the same set of input options that are present in REST, where one can choose the different structures and associated physical parameters.

2. Rough Ellipsoid Structure Tools (REST)

The REST package is a FORTRAN package wrapped with a Java graphical user interface (GUI) that aims to generate computer models of realistic cosmic dust particles in the form of rough/irregular/broken/porous structures. REST is composed of three main parts: (1) the JAVA GUI takes the input parameters, (2) FORTRAN modules perform the calculations to craft roughness or break the initial spherical, superellipsoidal, or fractal aggregate structures, and (3) PYTHON3 scripts plot the respective structures using the VTK and PyVista[3] (Sullivan & Kaszynski 2019) python modules. REST uses the CALLTARGET module from DDSCAT (Draine & Flatau 1994) to generate the initial spherical and superellipsoidal structures.

The different input and output parameters of REST are shown below:

The input parameters are

1. Type of structure
   (a) Strongly damaged sphere (SDS)
   (b) Rough surface (RS)
   (c) Poked structure (PS)
   (d) Rough-surface superellipsoids (RS-SE)
   (e) Poked structure superellipsoids (PS-SE)
   (f) Rough fractal aggregates (RFA)
2. Radius for spherical initial structure or circumscribed sphere R_d
3. Initial number of dipoles N_d
4. Semiaxes a, b, and c of the initial superellipsoidal structure
5. East–west exponent e of the initial superellipsoidal structure
6. North–south exponent n of the initial superellipsoidal structure
7. Radii and coordinate points of each sphere of fractal aggregate (r, X,Y,Z)
8. Number of material seed cells N_m
9. Number of space seed cells N_s
10. Number of surface space seed cells N_{ss}
11. Thickness of the surface layer t
12. Final target file name.

The output parameters are

1. Initial and final DDSCAT structure target file
2. Initial and final VTK structure file
3. Structure plot png file.

The Java GUI asks the user to choose the type of structure and enter the respective input parameters such as size (radius in the case of SDS, RS, and PS structures; semiaxes and exponents in the case of RS-SE and PS-SE structures), number of material seed cells, number of internal space seed cells, and/or number of surface seed cells. In the case of RFA structures, the applications asks the user to choose the structure file of an FA structure having the radii, coordinates, and composition tag of each sphere/monomer. After entering the input parameters, the user can proceed for calculation by clicking the "Calculate" button in the Java GUI. In each case, the base structure is a sphere. For SDS, RS, and PS, the radius of the initial sphere is R_d, while in the case of RS-SE and PS-SE the radius of the initial sphere is equal to the largest semiaxes. In the case of RFA structures, the radius of the initial sphere is equivalent to the radius of the FA structure. The initial spherical and superellipsoidal structures are generated using the CALLTARGET module considering the radius coming out from the input parameters discussed above. The initial and the final structure files are composed of seven columns, one for the dipole number (JA), three for the dipole coordinates (IX, IY, IZ) and the remaining three for the respective composition tags [ICOMP(x,y,z)]. The SDS, RS, and PS structures discussed below are generated following Zubko et al. (2006) and the structures RS-SE, PS-SE, and RFA are generated using algorithms that are discussed in this study for the first time. Figure 1 shows the flow diagram of the package showing the workflow of the six FORTRAN modules explained below.

2.1. Strongly Damaged Sphere (SDS)

The SDS is a kind of structure that has been broken from certain portion of its volume, yet retains a partial spherical shape. To generate an SDS structure REST follows the steps stated below:

1. Generate an initial spherical structure file `target.out` having N_d dipoles and radius R (in number of dipoles) using the `CALLTARGET` module.
2. Randomly choose N_m number of material seed cells from the N_d dipoles present in the `target.out` file.
3. Randomly choose N_s number of space seed cells from the N_d dipoles present in the `target.out` file.
4. Measure the distance $D_m^{i,j}$ between the jth material seed cell and ith dipole of the base structure, where $j = 1$ to N_m and $i = 1$ to N_d.
5. Measure the distance $D_s^{i,k}$ between the kth space seed cell and ith dipole of the base structure, where $k = 1$ to N_s and $i = 1$ to N_d.
6. Print those dipoles for which, $D_m^i < D_s^i$ in the final structure file.

[1] https://rest-package.readthedocs.io/
[2] https://form.jotform.com/drprithishhalder/rough-ellipsoid-structure-tools
[3] https://www.pyvista.org/

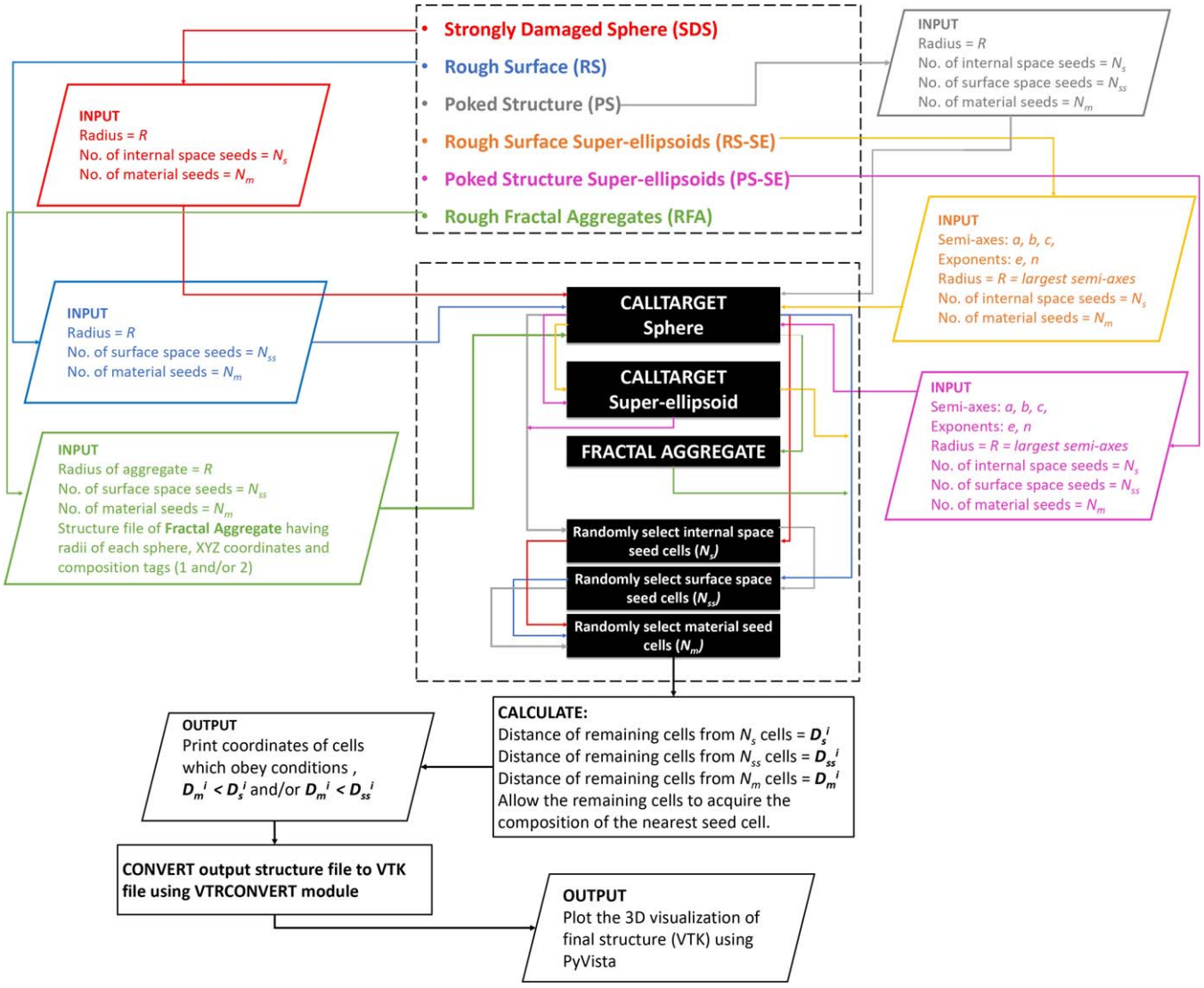

Figure 1. Flow diagram of the REST package.

The development of an SDS structure is shown in Figure 2. REST has two options for selecting seed cells for an SDS structure, (i) `Default seeds` and (ii) `Custom seeds`.

2.2. Rough Surface (RS)

The RS structures are spherical structures having a rough surface. Unlike SDS, the space seed cells in RS structures are selected on the surface of the base structure having a certain amount of thickness. To generate an RS structure REST follows the algorithm stated below:

1. Generate an initial spherical structure file `target.out` having N_d dipoles and radius R (in number of dipoles) using the `CALLTARGET` module.
2. Randomly choose N_m number of material seed cells from the N_d dipoles present in the `target.out` file.
3. Randomly choose N_{ss} number of surface space seed cells from the N_d dipoles present in the `target.out` file. The surface thickness should be $t \times r$.
4. Measure the distance $D_m^{i,j}$ between the jth material seed cell and ith dipole of the base structure, where $j = 1$ to N_m and $i = 1$ to N_d.
5. Measure the distance $D_{ss}^{i,l}$ between the lth surface space seed cell and ith dipole of the base structure, where $l = 1$ to N_{ss} and $i = 1$ to N_d.
6. Print those dipoles for which $D_m^i < D_{ss}^i$ in the final structure file.

The development of an RS structure is shown in Figure 3.

2.3. Poked Structures (PS)

The PS are structures that are poked from inside as well as from the surface. For PS, two types of space seeds are selected, one for the internal space and the other for the surface space. To generate a PS REST follows the algorithm stated below:

1. Generate an initial spherical structure file `target.out` having N_d dipoles and radius R (in number of dipoles) using the `CALLTARGET` module.
2. Randomly choose N_m number of material seed cells from the N_d dipoles present in the `target.out` file.
3. Randomly choose N_{is} number of internal space seed cells from the N_d dipoles present in the `target.out` file.

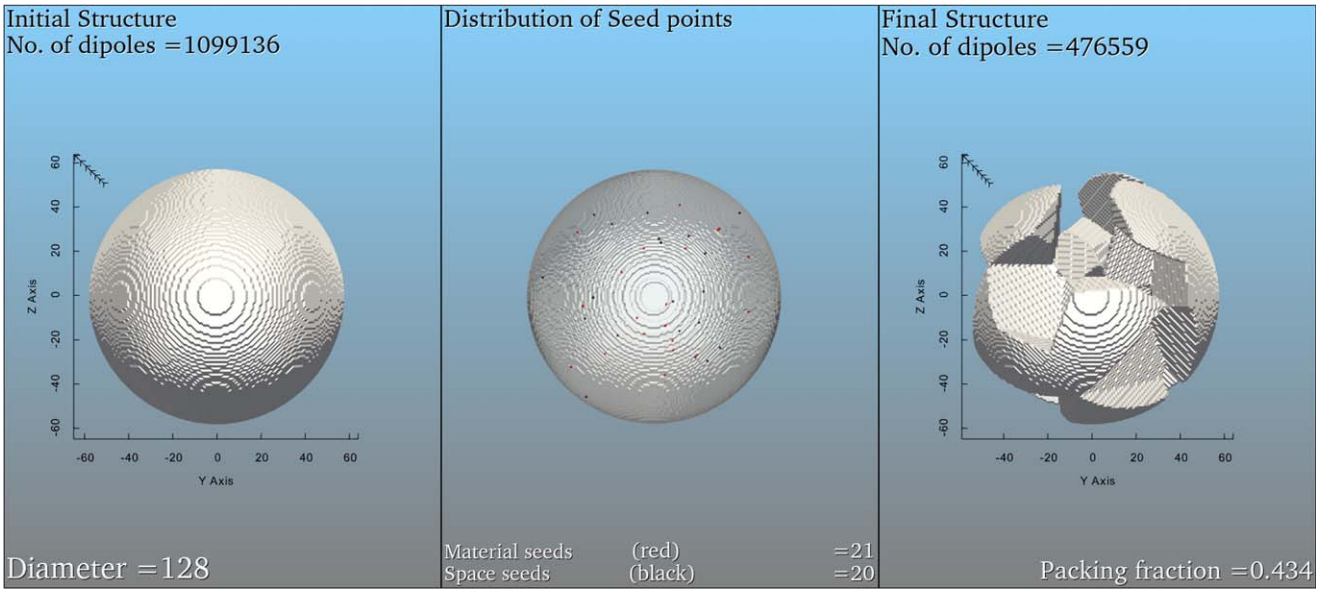

Figure 2. 3D visualization of an SDS (default) structure using REST (PyVista module).

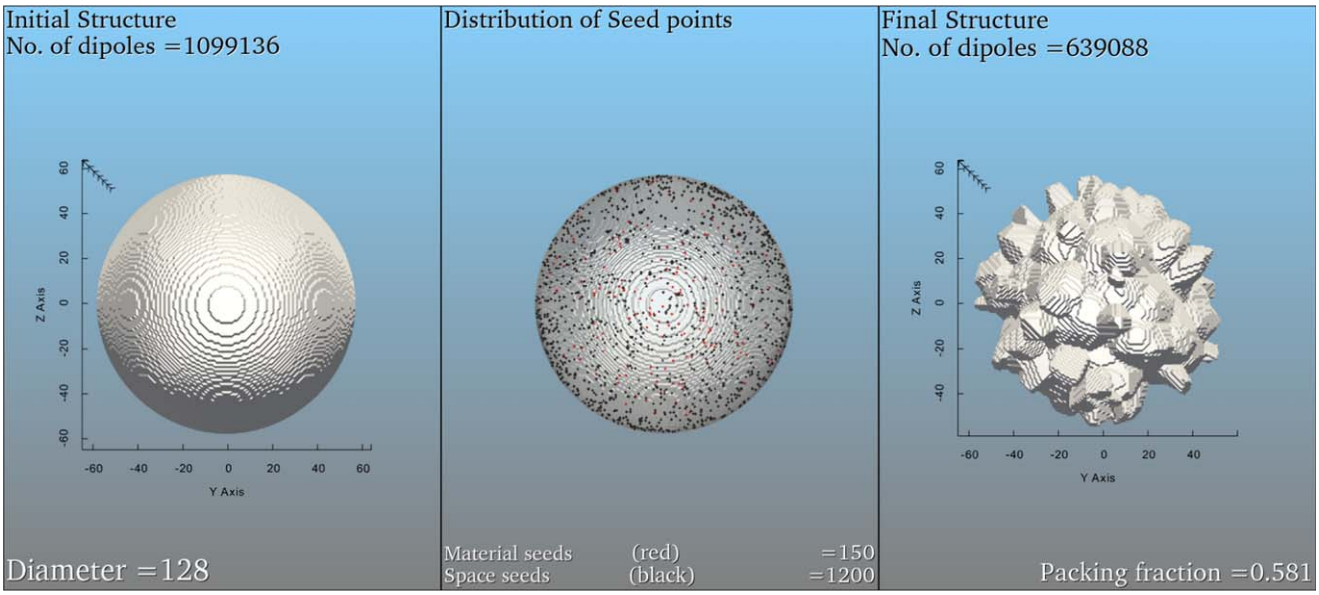

Figure 3. 3D visualization of an RS structure using REST (PyVista module).

4. Randomly choose N_{ss} number of surface space seed cells from the N_d dipoles present in the `target.out` file. The surface thickness should be $t \times r$.
5. Measure the distance $D_m^{i,j}$ between the jth material seed cell and ith dipole of the base structure, where $j = 1$ to N_m and $i = 1$ to N_d.
6. Measure the distance $D_{is}^{i,k}$ between the kth internal space seed cell and ith dipole of the base structure, where $k = 1$ to N_{is} and $i = 1$ to N_d.
7. Measure the distance $D_{ss}^{i,l}$ between the lth surface space seed cell and ith dipole of the base structure, where $l = 1$ to N_{ss} and $i = 1$ to N_d.
8. Print those dipoles for which $D_m^i < D_{is}^i$ and $D_m^i < D_{ss}^i$ in the final structure file.

The development of a PS structure is shown in Figure 4.

The PS option asks the user to choose from a homogeneous and inhomogeneous morphology. In the case of a homogeneous morphology REST takes material seeds for one kind of material, while in the case of an inhomogeneous morphology, REST takes two kinds of material seeds, N_{m1} and N_{m2}. Thus the overall material seeds $N_m = N_{m1} + N_{m2}$.

2.4. Rough Superellipsoids

Rough superellipsoids are superellipsoidal structures having a rough or irregular surface or volume morphology. Superellipsoids are generalized ellipsoidal structures that are defined by the following equation (Faux & Pratt 1979; Barr 1981; Bi et al. 2018):

$$\left[\left(\frac{x}{a}\right)^{2/e} + \left(\frac{y}{b}\right)^{2/e}\right]^{e/n} + \left[\left(\frac{z}{c}\right)\right]^{2/n} = 1 \quad (1)$$

where a, b, and c are the semiaxes of the superellipsoidal structure along the x, y, and z directions in Cartesian coordinates. The

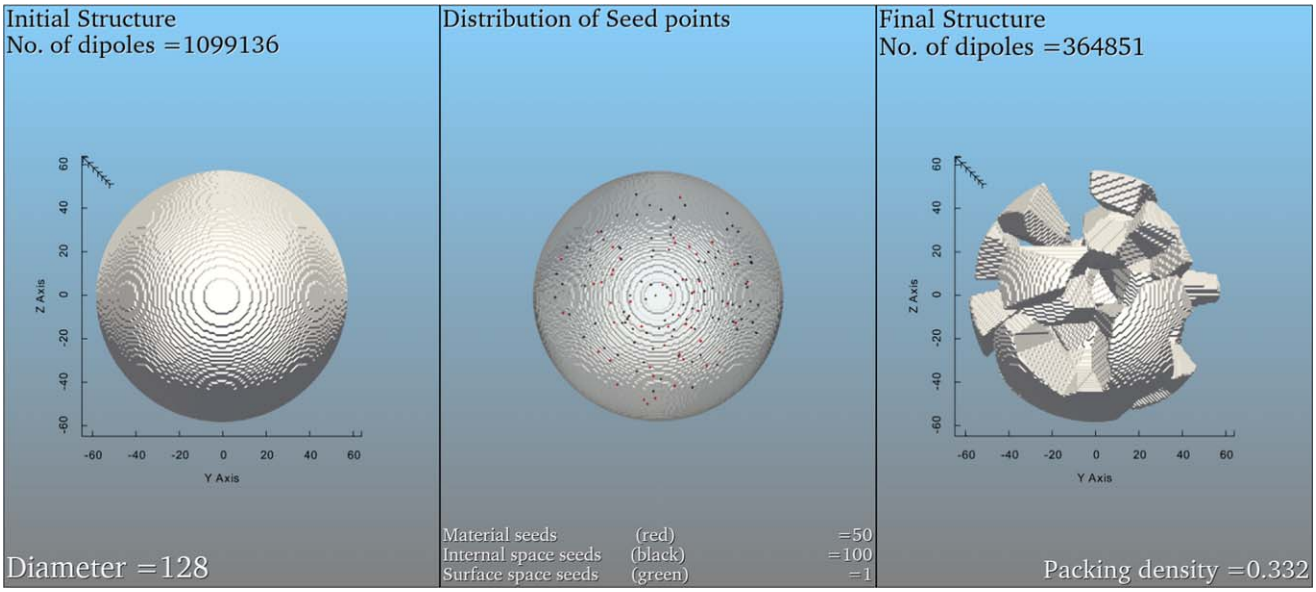

Figure 4. 3D visualization of PS using REST (PyVista module).

parameters e and n in Equation (1) are the east–west and north–south exponents of the superellipsoidal structure (also called roundness parameters). The roundness parameters determine the structural variation for a constant aspect ratio (a/b or b/c).

REST uses superellipsoids (SE) as base structures to create RS-SE and PS-SE. To generate RS-SE/PS-SE structures REST uses the following algorithm:

1. Generate the initial SE structure having N_d dipoles and semiaxes a, b, and c (in number of dipoles) using the `SUPELLIPS` function from the `CALLTARGET` module.
2. Create a circumscribed sphere having radius $R =$ longer semiaxis of an initial SE structure using the `ELLIPSOID` function from the `CALLTARGET` module.
3. Randomly choose N_{ss} surface space seed cells from the boundary where the surface of SE meets that of the circumscribed sphere.
4. Randomly choose N_m material seed cells from within the volume of the SE.
5. Measure the distance $D_m^{i,j}$ between the jth material seed cell and ith dipole of the base structure, where $j = 1$ to N_m and $i = 1$ to N_d.
6. Measure the distance $D_{ss}^{i,k}$ between the kth surface space seed cell and ith dipole of the base structure, where $k = 1$ to N_{ss} and $i = 1$ to N_d.
7. Print those dipoles for which $D_m^i < D_{ss}^i$ in the final structure file.
8. For the PS-SE structure randomly choose N_{is} internal space seed cells from the boundary where the surface of the SE meets that of the circumscribed sphere along with the abovementioned steps.
9. Measure the distance $D_{is}^{i,k}$ between the kth internal space seed cell and ith dipole of the base structure, where $k = 1$ to N_{is} and $i = 1$ to N_d.
10. Print those dipoles for which $D_m^i < D_{is}^i$ and $D_m^i < D_{ss}^i$ in the final structure file.

The development of RS-SE and PS-SE structures are shown in Figures 5 and 6, respectively.

2.5. Rough Fractal Aggregates (RFA)

The RFA are fractal aggregates made up of clusters of irregular rough-surface grains/monomers/subunits. The IDPs obtained from the Earth's stratosphere indicate the presence of an FA of irregular rough-surface grains. REST converts the smooth spherical surface of each sphere of a particular FA/cluster of spheres into rough- and irregular-surface grains or monomers. The following algorithm allows REST to craft RFA structures from FA structures made up of spheres:

1. Browse and select the structure file of an FA/cluster of spheres having the following format (i, R, X Y Z, $m$tag, $m$tag), where i is the sphere number, R is the ith sphere radius (in microns), X, Y, Z are the coordinates of each sphere (monomer) and the $m$tag is the composition tag.
2. Multiply each coordinate and radii with an integer scale factor n.
3. Measure the distance (d_{mono}) of each monomer from the center (0,0,0).
4. Create the initial sphere having N_d dipoles and radius $R_d =$ `maximum` (d_{mono}) (in number of dipoles) from the center of the initial sphere.
5. Randomly choose N_{ss} surface seed cells on the surface of the FA inside the initial sphere.
6. Randomly choose N_m material seed cells inside the surface of the FA.
7. Measure the distance $D_m^{i,j}$ between the jth material seed cell and ith dipole of the base structure, where $j = 1$ to N_m and $i = 1$ to N_d.
8. Measure the distance $D_{ss}^{i,k}$ between the kth surface space seed cell and ith dipole of the base structure, where $k = 1$ to N_{ss} and $i = 1$ to N_d.
9. Print those dipoles for which $D_m^i < D_{ss}^i$ in the final RFA structure file.

The development of an RFA structure is shown in Figure 7.

The RFA structure generated using REST retains the fractal nature from the initial FA or cluster of spheres. The roughness

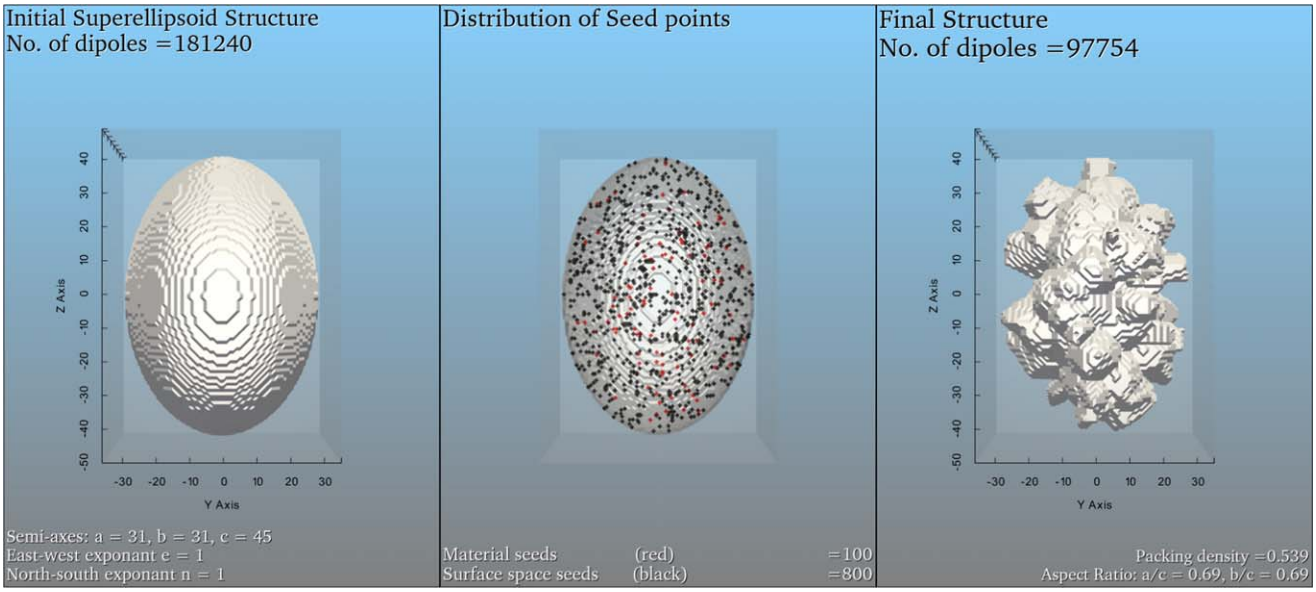

Figure 5. 3D visualization of an RS-SE structure using REST (PyVista module).

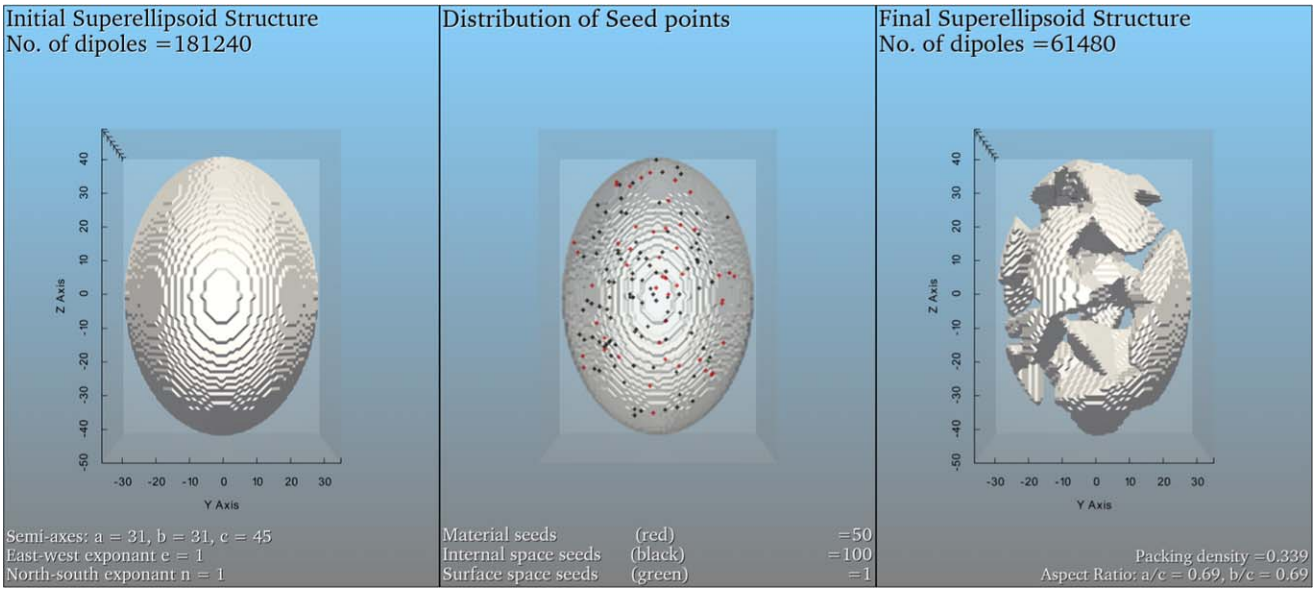

Figure 6. 3D visualization of a PS-SE structure using REST (PyVista module).

crafted on the final structure induces a certain amount of porosity that can be controlled by changing the ratio of material and space seed cells (N_m:N_{ss}). The RFA structure is a unique structure and holds a very close resemblance in terms of structural morphology with the structures of IDPs obtained from the Earth's stratosphere and the Stardust mission.

2.6. Inhomogeneous Structures

REST allows users to choose from homogeneous and inhomogeneous morphologies. In the case of a homogeneous morphology REST takes material seeds for one kind of material as explained in the earlier subsections, while in the case of an inhomogeneous morphology, it takes two kinds of material seeds, N_{m1} and N_{m2}. Thus, the overall material seeds $N_m = N_{m1} + N_{m2}$. The inhomogeneous option is available for the structure modules PS, PS-SE, and RFA. Figures 8–10 show the construction of respective inhomogeneous structures.

3. Physical Parameters

The development of the structures discussed in Section 2 deals with the geometry of the dipole matrix generated using the CALLTARGET function. The units of all the parameters in the algorithm are based on the number of dipoles. Hence, in this section the associated physical parameters of the structures and their units are discussed.

3.1. Radius

In REST the radius R_d or the semiaxes a, b, and c must be chosen in terms of the number of dipoles from the origin to the surface. If $R_d = 32$ (number of dipoles from the origin to the surface), then diameter $= 64$ and $N_d = 137{,}376$. In

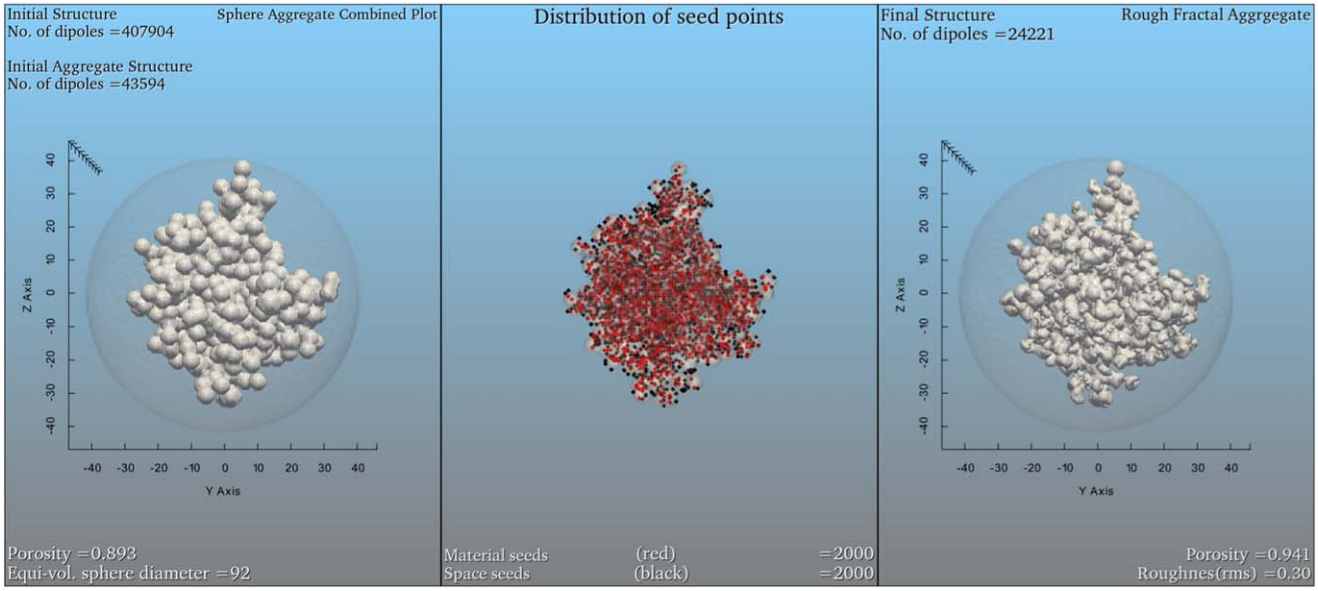

Figure 7. 3D visualization of an RFA structure using REST (PyVista module).

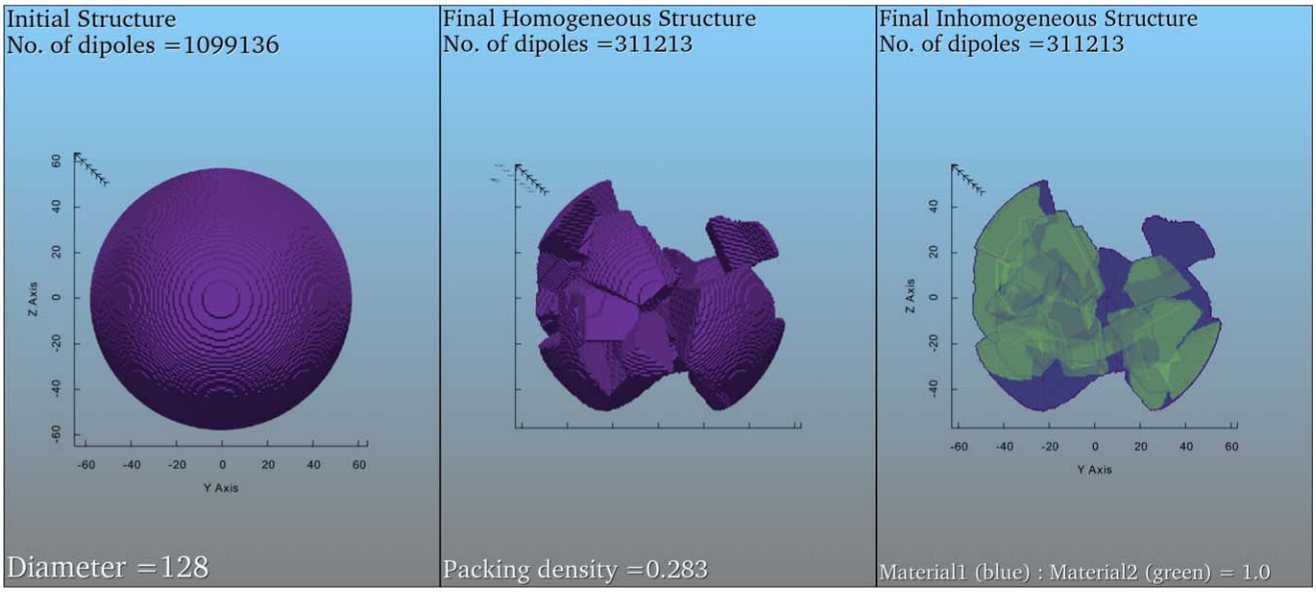

Figure 8. 3D visualization of inhomogeneous PS structures using REST (PyVista module).

light-scattering calculations the size parameter X of a particle is used to solve the scattering problem. X is defined by the following equation,

$$X = \frac{2\pi R}{\lambda}, \tag{2}$$

where R is the radius (in physical units) and λ is the wavelength of incident radiation (in physical units). Follow Table 1 to choose the value of radius R_d (in number of dipoles) (Zubko et al. 2020) or semiaxes.

For example, if $R = 1.0\ \mu$m, $\lambda = 0.450\ \mu$m, then

$$X = \frac{2\pi R}{\lambda} = \frac{2 \times 3.142 \times 1.0}{0.450} = 13.96 < 16.$$

As $X < 16$, the radius in dipoles $R_d = 32$.

This procedure for selection of the radius is for better coverage of mesh or dipoles so that the DDSCAT calculation accuracy is better. One can always use radius of their choice, but calculation accuracy may decrease if the values decrease from those shown in Table 1.

3.2. Semiaxes

In superellipsoid options, REST takes the semiaxes a, b, and c as inputs for the size or dimension of the initial superellipsoid structure. For particles with a size parameter $X < 16$, N_d of the final structure should be within 20,000–40,000 for better accuracy. In the case of a superspheroid structure, $a = b$ and a/c is the aspect ratio.

3.3. Bulk Density

The bulk density ρ_b of a material is defined by the following equation,

$$\rho_f = \frac{\rho_b}{\rho}, \tag{3}$$

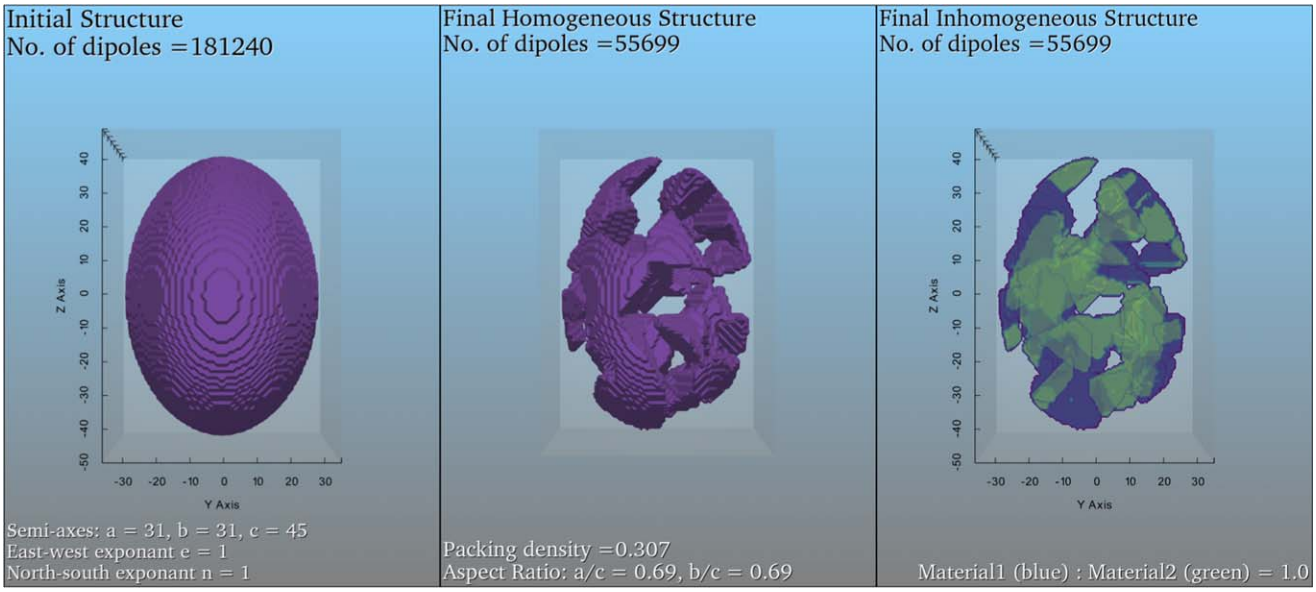

Figure 9. 3D visualization of an inhomogeneous PS-SE structure using REST (PyVista module).

where ρ_f and ρ are the packing fraction and true density of the material, respectively. The packing fraction ρ_f of a material is the fraction of space occupied by the atoms/the unit cells, in this case its dipoles.

In REST, the value of ρ_f is determined by the following equation,

$$\rho_f = \frac{\texttt{Volume of final structure}}{\texttt{Volume of initial structure}} = \frac{V_f}{V_i} = \frac{N_d(\texttt{final}) \times d^3}{N_d(\texttt{initial}) \times d^3} = \frac{N_d(\texttt{final})}{N_d(\texttt{initial})}, \quad (4)$$

where $N_d(\texttt{initial})$ and $N_d(\texttt{final})$ are the total number of dipoles in the initial and the final structure, respectively, while d is the dipole spacing. In DDSCAT the volume of a structure is determined by the number of dipoles N_d and the dipole spacing d,

$$V = N_d \times d^3. \quad (5)$$

Thus, for an RS particle having radius $r = 32$, $N_d(\texttt{initial}) = 137{,}376$, $N_d(\texttt{final}) = 71{,}813$, the packing fraction is

$$\rho_f = \frac{N_d(\texttt{final})}{N_d(\texttt{initial})} = \frac{71,\,813}{137,\,376} = 0.523.$$

The study of comet dust particles collected from the Stardust mission reveals a bulk density in the range 0.3–3.0 g cm^{-3}, with highly porous particles having a bulk density as low as 0.3 g cm^{-3} and less porous/solid particles having a bulk density as high as 3.0 g cm^{-3} (Hörz et al. 2006). The values of ρ_f for the different structures obtained using REST are shown in Figure 11.

3.4. Porosity

Porosity is one of the significant physical parameters for the RFA structures. The degree of porosity is defined by the ratio of the total number of space seed cells in the entire volume circumscribing the RFA structure by the total volume of the circumscribing sphere. Thus, we have

$$\texttt{Volume of initial structure}(V_i) = N_d(\texttt{initial}) \times d^3$$
$$\texttt{Volume of final structure}(V_f) = N_d(\texttt{final}) \times d^3.$$

The total volume of space seed cells is given by

$$V_T = [N_d(\texttt{final}) - N_d(\texttt{initial})] \times d^3.$$

Therefore, the degree of porosity is

$$P = \frac{V_T}{V_f} = \frac{[N_d(\texttt{final}) - N_d(\texttt{initial})] \times d^3}{N_d(\texttt{final}) \times d^3} = \frac{[N_d(\texttt{final}) - N_d(\texttt{initial})]}{N_d(\texttt{final})}. \quad (6)$$

3.5. Roughness

In this study, the surface roughness of each monomer/grain of an RFA particle is defined as the mean deviation of the surface normal of an RFA grain or monomer from the initial spherical grain of the initial FA/cluster of spheres. If D_i is the distance of the ith dipole or lattice point on the jth RFA monomer/grain from the center of the jth RFA monomer/grain, then the roughness on the jth monomer/grain is defined by the rms equation

$$R^j_{\rm rms} = \left\{\frac{1}{N_j}\sum_{n=1}^{N_j}(D_i - \langle D_i\rangle)^2\right\}^{1/2}. \quad (7)$$

4. Applications

In this section, some of the applications of REST that can be employed to create visually realistic cosmic dust particles are discussed. AD, AD superellipsoids (AD-SE) and RFA-AD mixed-morphology particles are generated using REST. The respective particles are used to simulate light scattering using DDSCAT to calculate the the degree of linear polarization for a changing phase angle and size parameter considering a different material composition. The light-scattering parameters are defined by the phase matrix that represents a far-field

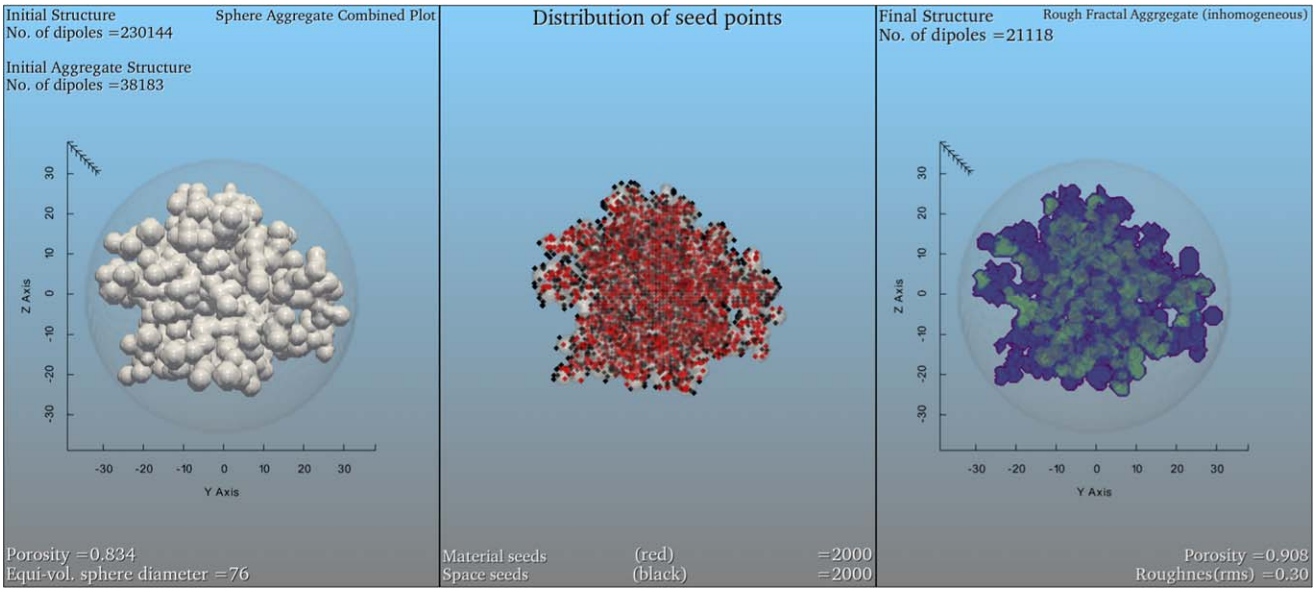

Figure 10. 3D visualization of an inhomogeneous RFA structure using REST (PyVista module).

Table 1
Table to Choose the Radius in Number of Dipoles according to the Required Size Parameter (X)

X	Radius (R_d)	Diameter	N_d
$X < 16$	32	64	137,376
$X = 16$–32	64	128	1,099,136
$X > 32$	128	256	8,783,848

transformation of the Stokes parameters of the incident light (I_i, Q_i, U_i, V_i) to that of the scattered light (I_s, Q_s, U_s, V_s). This phase matrix is given by Bohren & Huffman (1998):

$$\begin{pmatrix} I_s(\theta) \\ Q_s(\theta) \\ U_s(\theta) \\ V_s(\theta) \end{pmatrix} = \frac{1}{k^2 d^2} \begin{pmatrix} S_{11}(\theta) & S_{12}(\theta) & S_{13}(\theta) & S_{14}(\theta) \\ S_{21}(\theta) & S_{22}(\theta) & S_{23}(\theta) & S_{24}(\theta) \\ S_{31}(\theta) & S_{32}(\theta) & S_{33}(\theta) & S_{34}(\theta) \\ S_{41}(\theta) & S_{42}(\theta) & S_{43}(\theta) & S_{44}(\theta) \end{pmatrix} \times \begin{pmatrix} I_i(\theta) \\ Q_i(\theta) \\ U_i(\theta) \\ V_i(\theta) \end{pmatrix} \quad (8)$$

where k is the wavenumber, d is the distance between the scatterer and the observer, and S_{ij} represents the scattering matrix elements. Angle θ is the scattering angle, $\theta = [0°, 180°]$.

The degree of linear polarization explained below to denote the light-scattering behavior of the respective particles is defined by $-S_{12}/S_{11}$.

4.1. Agglomerated Debris (AD)

The AD particles are the model cosmic dust particles that are most widely used by different researchers to model the light-scattering properties of comet dust, asteroid dust, and dust in debris disks. The AD particles have a highly irregular morphology with their shape and bulk density resembling those of the solid or less porous group of particles found in comets. These particles require a relatively smaller number of free parameters to simulate light scattering by cosmic dust. The AD particles are generated using the following parameters considering the PS algorithm:

1. R_d (in number of dipoles) $= 64$
2. $N_m = 21$
3. $N_{is} = 20$
4. $N_{ss} = 100$
5. $t = 1\%$.

Figure 12 shows the AD structure formed using the above parameters. The initial spherical structure has $N_d = 1{,}099{,}136$ and the final AD structure has $N_d = 286{,}886$ with the packing fraction $\rho_f = 0.261$. Figure 13 shows the inhomogeneous AD particles generated using REST considering the PS and inhomogeneous algorithm discussed in Section 2.6.

4.2. Agglomerated Debris Superellipsoids (AD-SE)

The AD-SE are agglomerated debris particles confined within a superellipsoidal volume and hence one can study the effect of aspect ratio. The dust particles present in a circumstellar or protoplanetary environment possess a certain order of aspect ratio and are believed to be oriented under the effect of a stellar magnetic field. To study the dust in such environments, the AD-SE particles shall provide better interpretation of the observed polarization and extinction. The AD-SE particles are generated using the following parameters considering the PS-SE algorithm:

1. Semiaxes: $a = 31$, $b = 31$, $c = 45$
2. Exponents: $n = 1$, $e = 1$
3. $N_m = 21$
4. $N_{is} = 20$
5. $N_{ss} = 100$.

Figure 14 shows the AD-SE structure formed using the above parameters. The initial SE structure has $N_d = 181{,}240$ and the final AD-SE structure has $N_d = 48{,}945$ with a packing fraction $\rho_f = 0.27$ and aspect ratio: $a/c = b/c = 0.69$. Figure 15 shows the inhomogeneous AD-SE particles generated using REST considering the PS-SE and inhomogeneous algorithm discussed in Section 2.6.

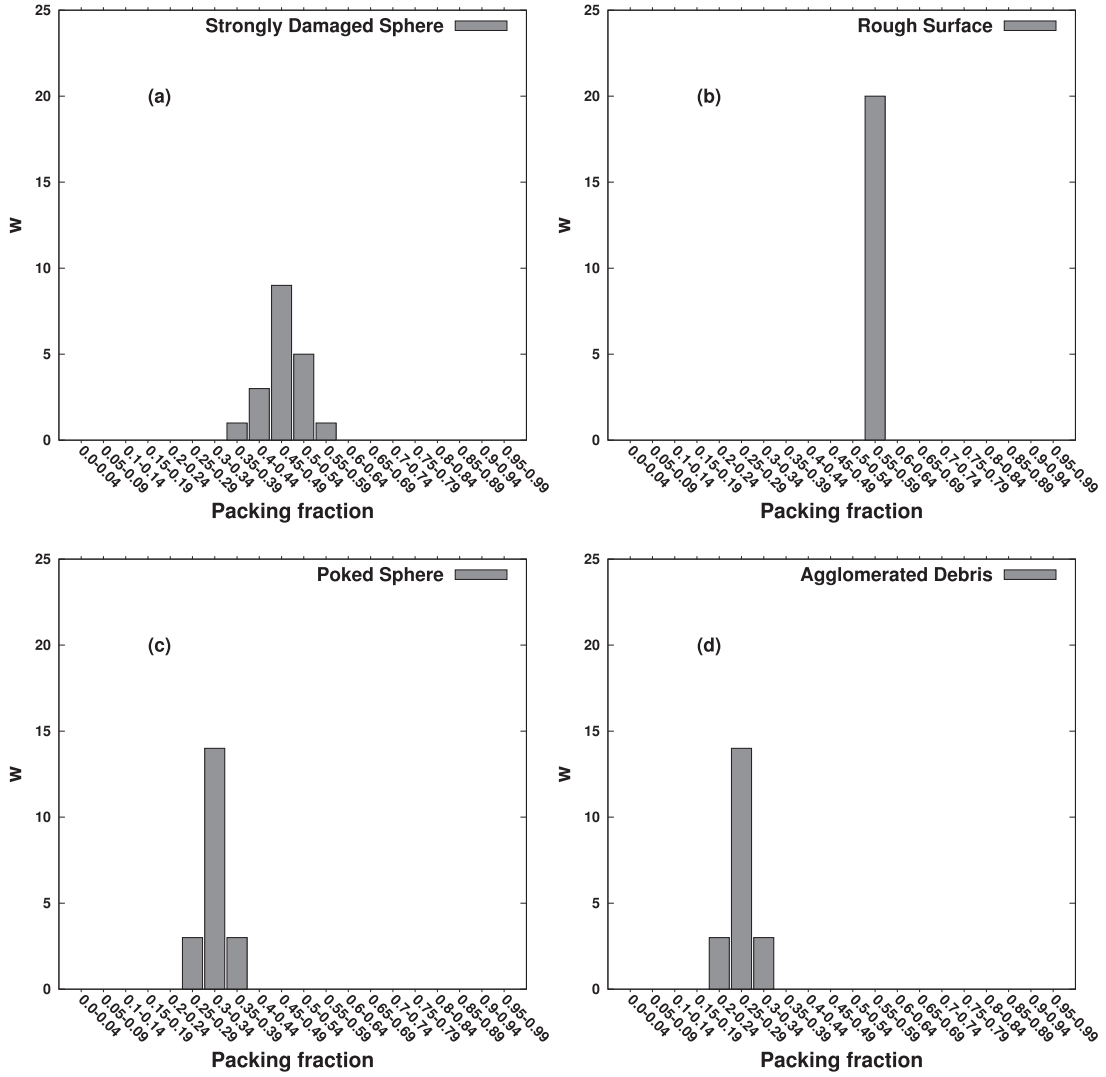

Figure 11. Packing fraction of different structures generated using REST.

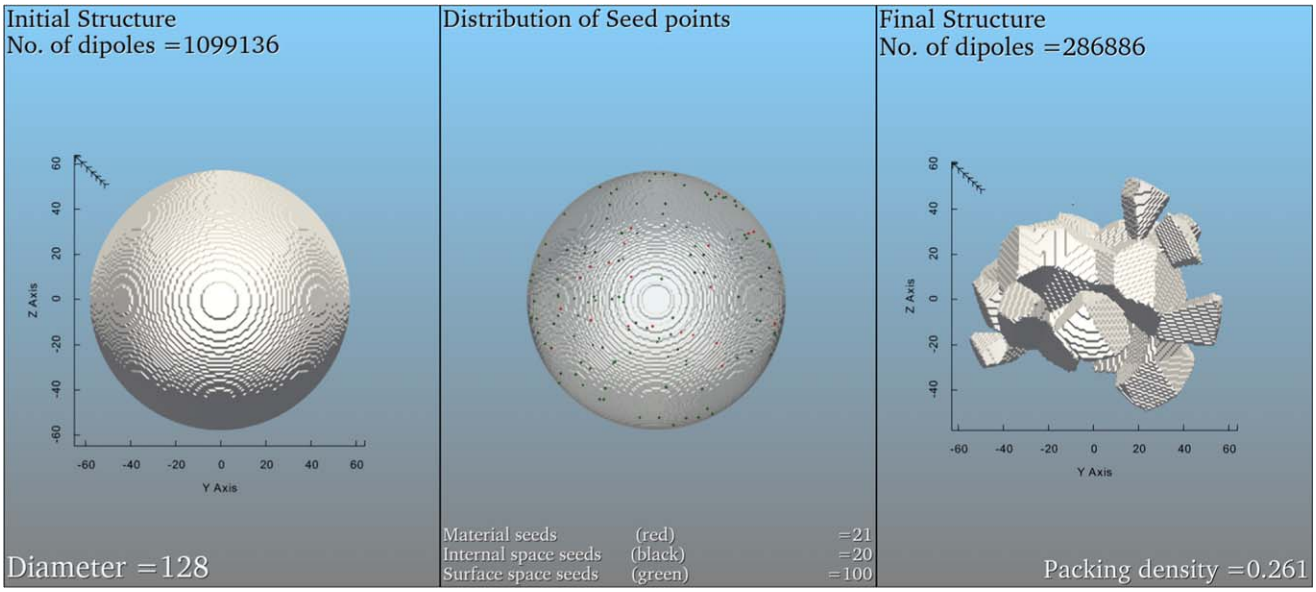

Figure 12. 3D visualization of an AD structure using REST (PyVista module).

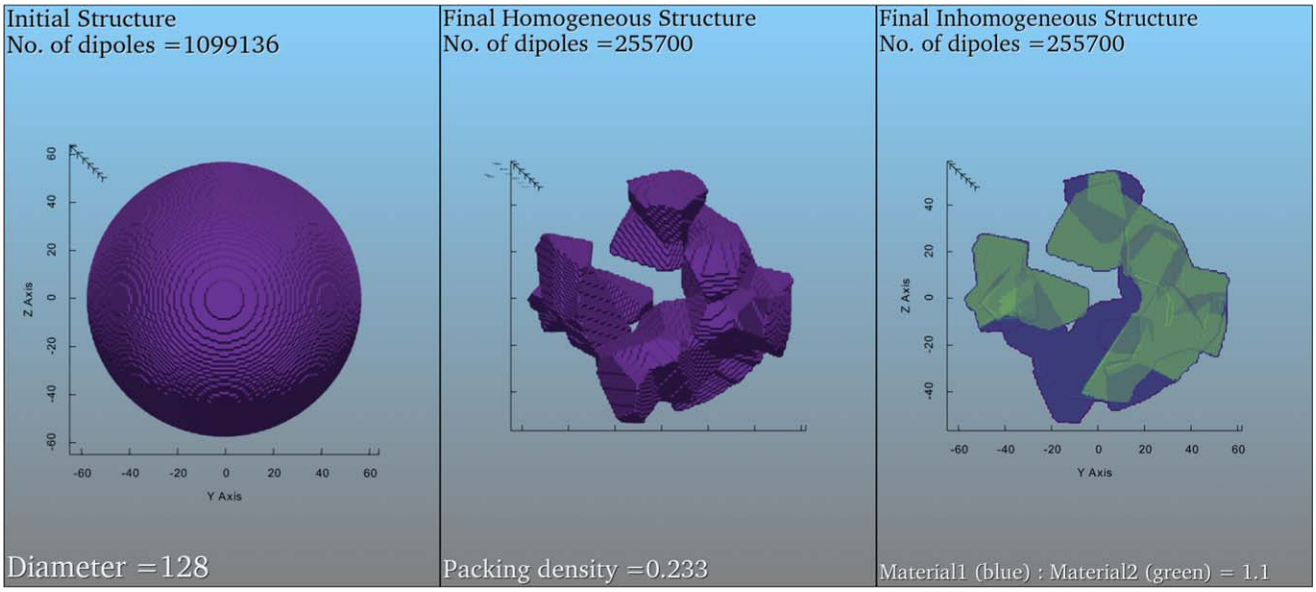

Figure 13. 3D visualization of an inhomogeneous AD structure using REST (PyVista module).

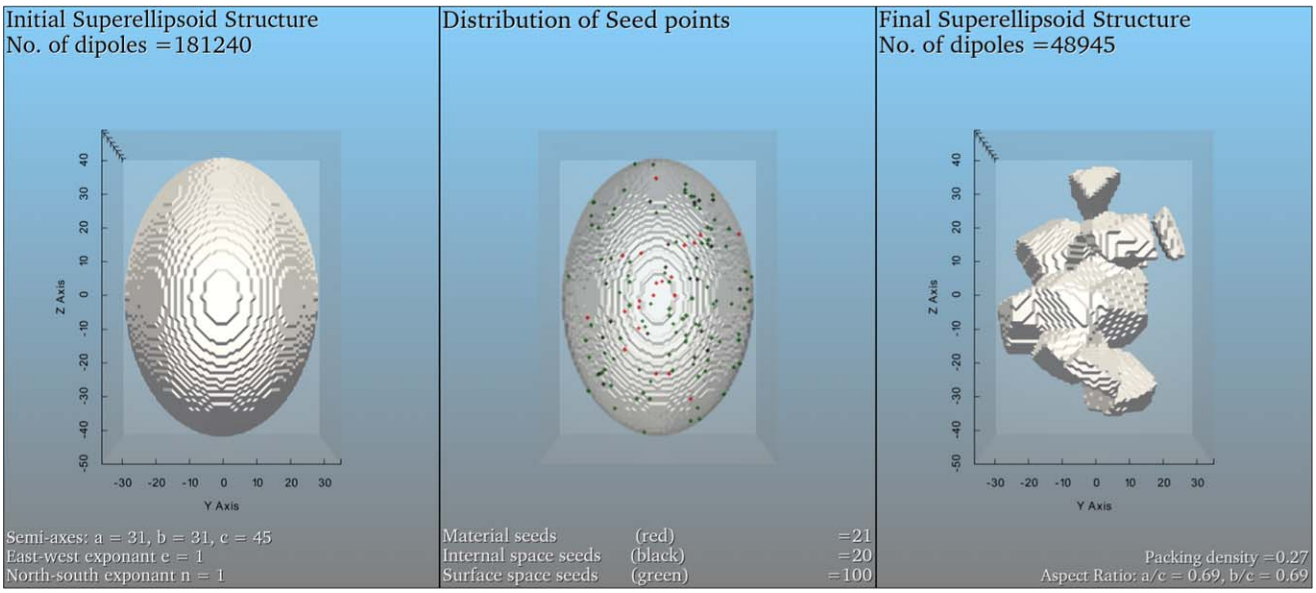

Figure 14. 3D visualization of an AD-SE structure using REST (PyVista module).

Figures 16(a)–(c) show the variation of the degree of linear polarization $(-S_{12}/S_{11})$ with increasing phase angle (0°–180°) over a size parameter ($x = 2\pi R/\lambda$) ranging from 2–16 for material compositions of ice, organics, and silicates. The results are similar to those obtained for AD particles in Zubko et al. (2006). Figures 16(d)–(f) show the variation of the degree of linear polarization $(-S_{12}/S_{11})$ with increasing phase angle (0°–180°) over a size parameter ($x = 2\pi R/\lambda$) ranging from 2–16 for material compositions of ice, organics, and silicates. The scattered light in the case of AD-SE is more depolarized compared to that obtained for AD particles for all the three compositions.

4.3. Mixed Morphology (RFA-AD)

As REST provides an opportunity to create numerous categories of particles, in this subsection the development of a new RFA-AD mixed morphology is discussed. In various dusty regions such as cometary coma, protoplanetary disks, and/or debris disks, there is high chance that particles of different morphologies may coexist as single entities. The significance of such complex morphologies are still unknown. Two structures, RFA (high porous) and AD (low porous), having different morphologies are created using REST and an algorithm (not included in REST) is developed to fit the AD structures within the pores of the RFA structure. Further, three RFA-AD structures having RFA:AD ratios of (90:10), (80:20), and (70:30) are created. Figures 17(a)–(c) show the variation of the degree of linear polarization $(-S_{12}/S_{11})$ with increasing phase angle (0°–180°) over a size parameter ($x = 2\pi R/\lambda$) ranging from 2–16 for the three different mixing ratios of RFA: AD where the composition of RFA is silicate while that of AD is ice.

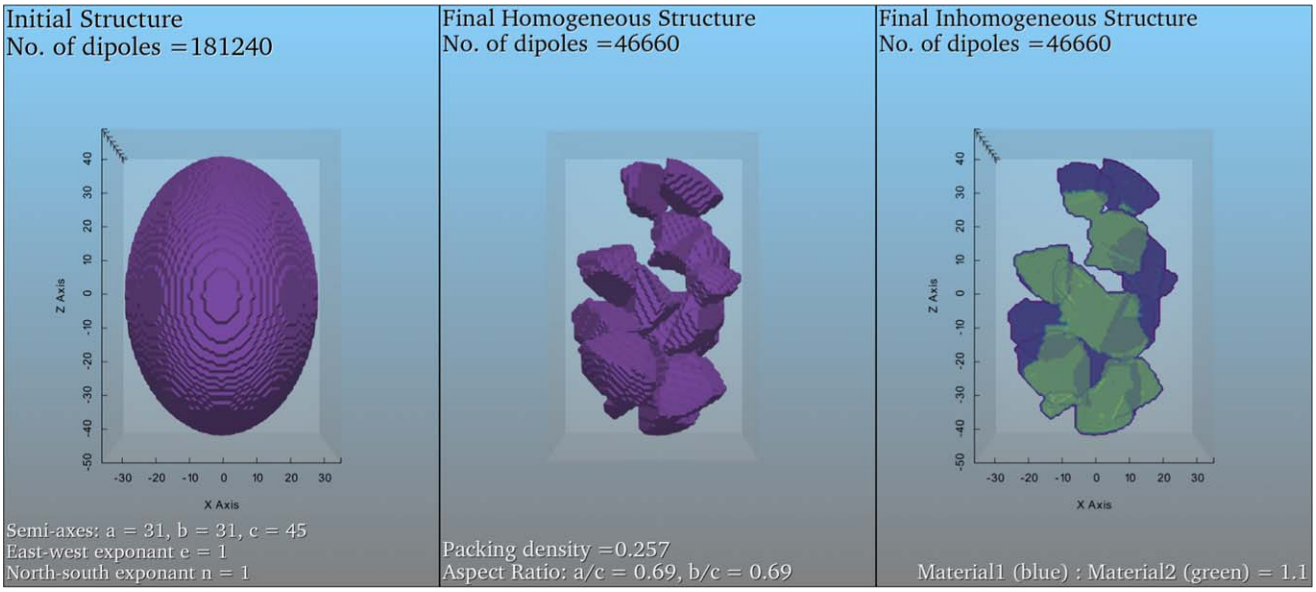

Figure 15. 3D visualization of an inhomogeneous AD-SE structure using REST (PyVista module).

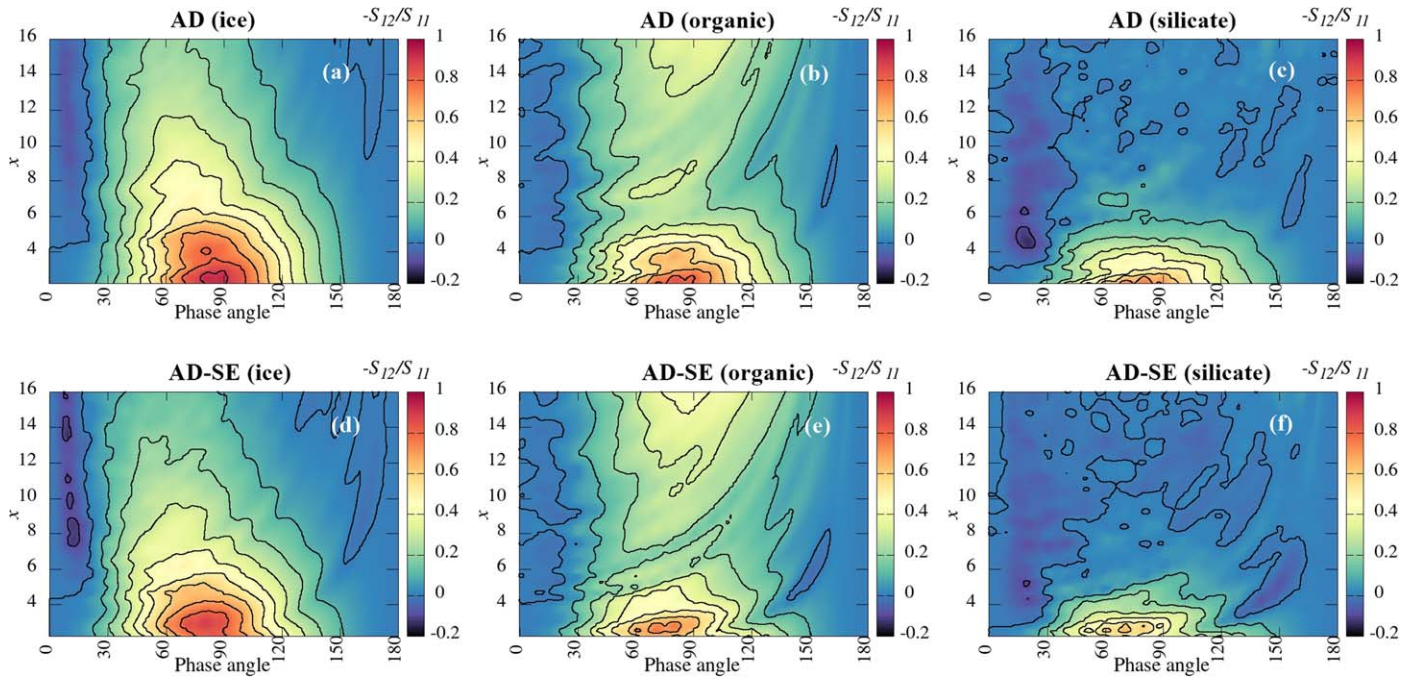

Figure 16. Variation of the degree of linear polarization with phase angle for $X = 2$–16 for AD structures having compositions of ice (a), organics (b), and silicate (c) and for AD-SE structures having compositions of ice (d), organics (e), and silicate (f).

To verify the computational accuracy of particles generated using REST, Figure 2 of Videen et al. (2015) is recreated, where the authors depict the degree of linear polarization and intensity obtained from light-scattering simulations over inhomogeneous AD particles having a mixture of two different refractive indices for three different combinations as shown in Table 2. To generate inhomogeneous AD particles the PS and inhomogeneous algorithms (explained in Section 2.2) are considered. Finally, light-scattering simulations are conducted for the three different combinations (15:6, 6:15, and 11:10) of refractive indices $(1.5+0i)$ and $(1.313+0i)$ for size parameter $x = 10$ over 2000 different orientations. Figure 18 shows that with an increase in the amount of ice from 25% to 75%, the maximum polarization increases, the minimum polarization remains unchanged, while the phase function (S_{11}) decreases.

5. Discussion and Conclusions

Following growing research in the field of dust in astrophysics and the measurements of IDPs and comet dust from Earth-based and in situ space missions, this study reports the development of a Java application package, Rough Ellipsoid Structure Tools (REST). The application generates irregular dust structures that are constrained by physical parameters such as size, bulk density, porosity, aspect ratio, and composition. These are the necessary parameters required for better interpretation of the light-scattering and thermal emission observations from different dusty sources.

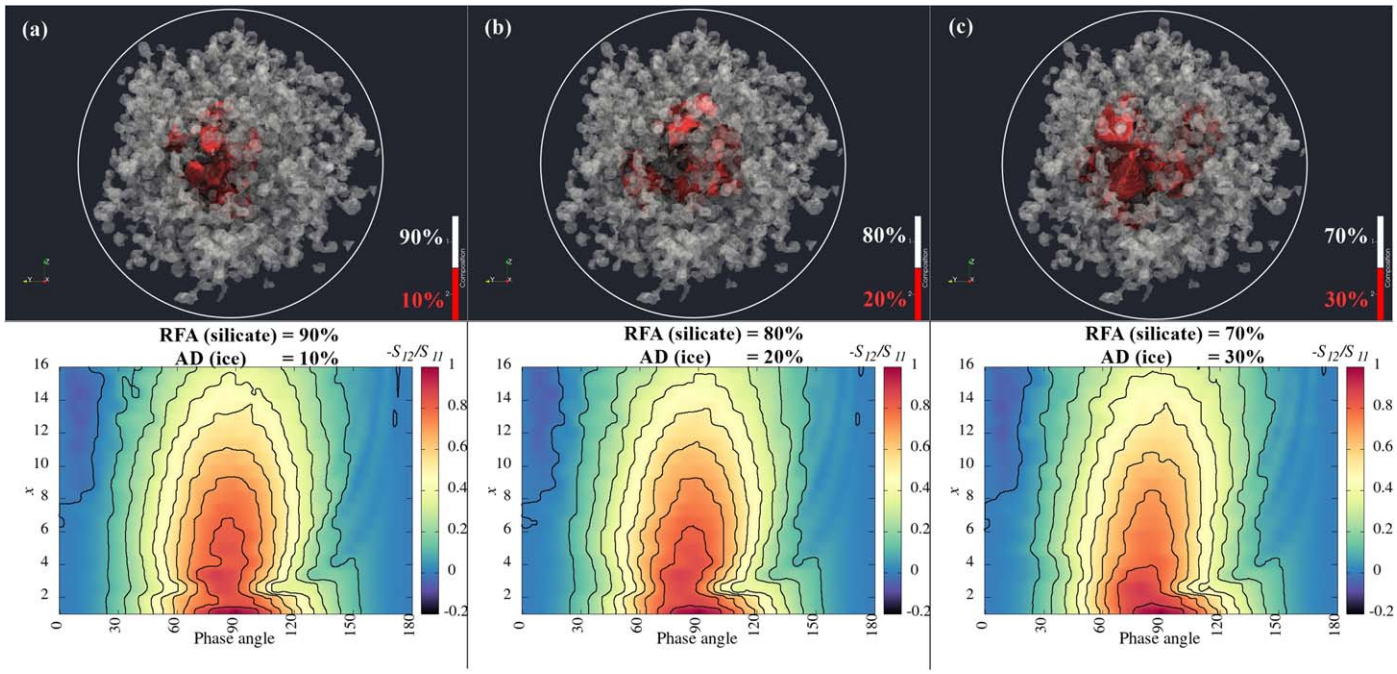

Figure 17. 3D visualization and respective variation in the degree of linear polarization with phase angle for $X = 2$–16 over mixed-morphology RFA-AD structures having mixing ratios (90:10) (a), (80:20) (b), and (70:30) (c).

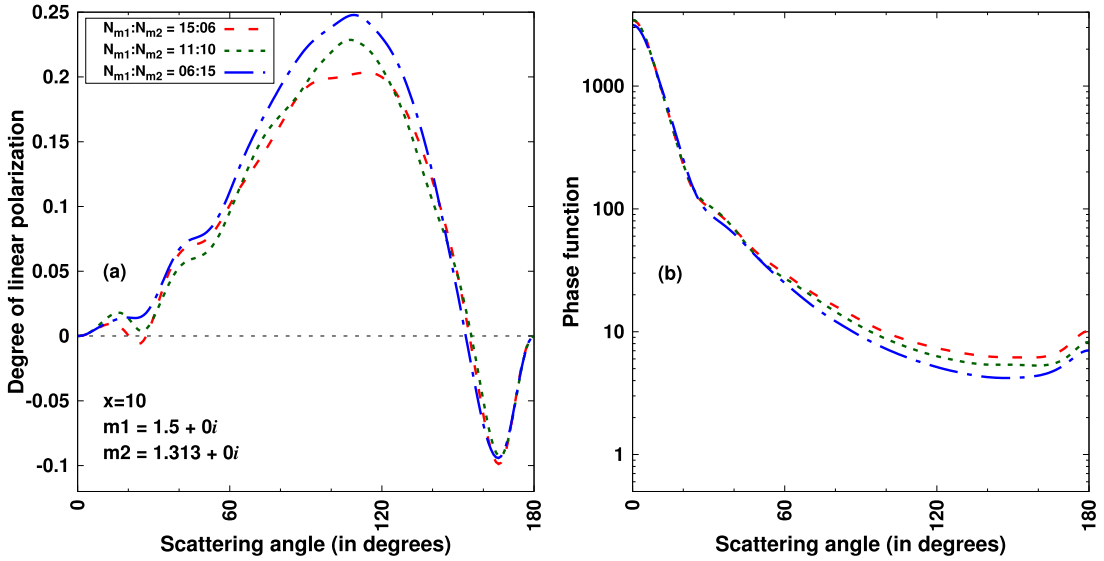

Figure 18. Verification of computational accuracy of the particles generated using REST: recreating the variation of the degree of linear polarization (a) and phase function (b) with scattering angle for inhomogeneous AD particles following Figure 2 from Videen et al. (2015).

Table 2
Three Different Combinations of Refractive Indices Used by Videen et al. (2015)

S/N	*m1*	*m2*	N_{m1}:N_{m2}
1	1.5+0*i*	1.313+0*i*	15:6
2	1.5+0*i*	1.313+0*i*	6:15
3	1.5+0*i*	1.313+0*i*	11:10

REST shall be very useful for generating pristine cosmic dust particles found in comets, protoplanetary disks, debris disks, and the interstellar medium. The morphology of RFA and AD structures generated using REST resembles those from the original samples of IDPs and comets and shall provide better interpretations. Further, the presence of aspect ratio in the superellipsoidal structures such as RS-SE, PS-SE, and AD-SE shall be useful to explain radiative-torque alignment in protoplanetary and circumstellar dust. The flexibility of REST to craft structures by controlling the number of different seed cells, aspect ratio, and exponents provides a high possibility to create numerous type of dust morphologies. Practically, REST can be applied in various areas of research that incorporate material or dust properties. In astrophysics, it can be applied in the study of dust present in our solar system (IDPs, comets, asteroids, lunar dust, etc.). The rough superellipsoids generated using REST have crucial implications in the study of the interstellar medium, where the dust particles are

believed to have a certain aspect ratio and are influenced by radiation pressure and the Galactic magnetic field.

The author acknowledges the high-performance computing facilities (NOVA) of the Indian Institute of Astrophysics, Bangalore, and Vikram-HPC of the Physical Research Laboratory, Ahmedabad, where all the intensive light-scattering simulations were conducted. The author acknowledges Prof. Sujan Sengupta of IIA, Bangalore and Dr. Shashikiran Ganesh of PRL, Ahmedabad for important discussions. The author also acknowledges Prof. B. T. Draine for making DDSCAT publicly available.

ORCID iDs

Prithish Halder https://orcid.org/0000-0002-1073-1419

References

Aravind, K., Halder, P., Ganesh, S., et al. 2022, Icarus, 383, 115042
Barr, A. H. 1981, IEEE Comput. Graph. Appl., 1, 11
Bekki, K. 2015, MNRAS, 449, 1625
Bi, L., Lin, W., Liu, D., & Zhang, K. 2018, OExpr, 26, 1726
Bi, L., Wang, Z., Han, W., Li, W., & Zhang, X. 2022, Front. Remote Sens., 3, 35
Bi, L., Yang, P., Kattawar, G. W., & Mishchenko, M. I. 2013, JQSRT, 116, 169
Bohren, C. F., & Huffman, D. R. 1998, Absorption and Scattering of Light by Small Particles (Weinheim: Wiley-VCH)
Bradley, J. P. 2007, in Treatise on Geochemistry, ed. H. D. Holland & K. K. Turekian (Oxford: Pergamon), 1.26
Brownlee, D. E. 1985, AREPS, 13, 147
Chatterjee, H., Bardhan, D., Pal, S. K., Yanase, K., & Ghosh, S. K. 2021, J. Phys. Chem. Lett., 12, 4697
Choudhury, N. R., Vilaplana, R., Botet, R., & Sen, A. K. 2020, P&SS, 190, 104974
Das, H. S., Paul, D., Suklabaidya, A., & Sen, A. K. 2011, MNRAS, 416, 94
Deb Roy, P., Halder, P., & Das, H. 2017, Ap&SS, 362, 209
Draine, B. T., & Flatau, P. J. 1994, JOSAA, 11, 1491
Faux, I. D., & Pratt, M. J. M. J. 1979, Computational Geometry for Design and Manufacture (Old Saybrook, CT: Ellis Horwood Ltd), 329
Güttler, C., Mannel, T., Rotundi, A., et al. 2019, A&A, 630, A24
Halder, P., Deb Roy, P., & Das, H. S. 2018, Icar, 312, 45
Halder, P., & Ganesh, S. 2021, MNRAS, 501, 1766
Hörz, F., Bastien, R., Borg, J., et al. 2006, Sci, 314, 1716
Kimura, H., Kolokolova, L., & Mann, I. 2006, A&A, 449, 1243
Kolokolova, L., Das, H. S., Dubovik, O., Lapyonok, T., & Yang, P. 2015, P&SS, 116, 30
Lawler, M. E., & Brownlee, D. E. 1992, Natur, 359, 810
Lin, W., Bi, L., & Dubovik, O. 2018, JGRD, 123, 13917
Mannel, T., Bentley, M. S., Boakes, P. D., et al. 2019, A&A, 630, A26
Mishchenko, M. I., Travis, L. D., & Mackowski, D. W. 1996, JQSRT, 55, 535
Muinonen, K., Väisänen, T., Martikainen, J., et al. 2019, J. Vis. Exp., 2019, e59607
Muñoz, O., Moreno, F., Guirado, D., et al. 2012, JQSRT, 113, 565
Noguchi, T., Ohashi, N., Tsujimoto, S., et al. 2015, E&PSL, 410, 1
Petrov, D., & Zhuzhulina, E. 2022, JQSRT, 289, 108298
Purcell, E. M., Pennypacker, C. R., Purcell, E. M., & Pennypacker, C. R. 1973, ApJ, 186, 705
Sullivan, C. B., & Kaszynski, A. A. 2019, JOSS, 4, 1450
Videen, G., Zubko, E., Sun, W., Shkuratov, Y., & Yuffa, A. 2015, JQSRT, 150, 68
Waterman, P. C. 1971, PhRvD, 3, 825
Yurkin, M. A., & Hoekstra, A. G. 2011, JQSRT, 112, 2234
Zhuzhulina, E., Petrov, D., Kiselev, N., Karpov, N., & Savushkin, A. 2022, JQSRT, 290, 108321
Zubko, E., Shkuratov, Y., Kiselev, N. N., & Videen, G. 2006, JQSRT, 101, 416
Zubko, E., Videen, G., Arnold, J. A., et al. 2020, ApJ, 895, 110